Journal of Nuclear Materials 378 (2008) 244–256

Contents lists available at ScienceDirect

Journal of Nuclear Materials

journal homepage: www.elsevier.com/locate/jnucmat

Performance of a buried radioactive high level waste (HLW) glass after 24 years

Carol M. Jantzen *, Daniel I. Kaplan, Ned E. Bibler, David K. Peeler, M. John Plodinec

Savannah River National Laboratory, Aiken, SC 29808, United States

ARTICLE INFO

Article history:
Received 31 March 2008
Accepted 2 June 2008

ABSTRACT

A radioactive high level waste glass was made in 1980 with Savannah River Site (SRS) Tank 15 waste. This glass was buried in a lysimeter in the SRS burial ground for 24 years. Lysimeter leachate data was available for the first 8 years. The glass was exhumed in 2004. The glass was predicted to be very durable and laboratory tests confirmed this. Scanning electron microscopy of the glass burial surface showed no significant glass alteration consistent with results of other laboratory and field tests. Radionuclide profiling for alpha, beta, and ^{137}Cs indicated that Pu was not enriched in the soil while ^{137}Cs and ^{90}Sr were enriched in the first few centimeters surrounding the glass. Lysimeter leachate data indicated that ^{90}Sr and ^{137}Cs leaching from the glass was diffusion controlled.

1. Introduction

The most important requirement for high-level waste (HLW) glass acceptance for disposal in a geological repository is the chemical durability. During the early stages of glass dissolution in a geological repository, near static conditions are expected to dominate. Under these conditions, a gel layer resembling a membrane forms on the glass surface through which ions exchange between the glass and the contacting groundwater. The hydrated gel layer exhibits acid/base properties which are manifested as the pH dependence of the thickness and nature of the gel layer. The gel layer has been determined to age into either clay mineral assemblages or zeolite mineral assemblages [1]. The formation of one phase preferentially over the other has been experimentally related to changes in the pH of the contacting solution and related to the relative amounts of Al^{+3} and Fe^{+3} in a waste glass. During laboratory studies the formation of clay mineral assemblages on the leached glass surface layers (lower pH environments and/or Fe^{+3}-rich waste glasses) caused the dissolution rate to remain diffusion controlled but slow to a long term ‘steady state’ rate [1]. The formation of zeolite mineral assemblages of the analcime type (higher pH environments and/or Al^{+3}-rich glasses) on the leached glass surface layers caused the dissolution rate to increase and return to the initial high forward rate [1–3].

The return to the forward dissolution rate is undesirable for long term performance of glass in a disposal environment. The return to the forward rate of dissolution raises additional questions about (1) how short term accelerated laboratory performance tests relate to long term performance in a disposal environment and (2) whether the forward rate of dissolution should be used for repository risk assessments which is the current practice in the United States [4,5].

The study of HLW glasses that have been buried for long periods of time in a disposal environment and/or natural analog studies may be the only ways to elucidate whether short term accelerated laboratory durability test performance and glass durability models are related to the long term durability and performance of a waste glass in a disposal environment. The nature of the leached layer formed, the overall glass dissolution, and the migration of both radioactive and non-radioactive species into the surrounding soil must all be assessed.

1.1. Field tests of simulated and alpha-doped HLW glasses

Many field tests of simulated (non-radioactive) HLW glass durability have been performed and reviews of the subject are available elsewhere [6–8]. These include but are not limited to burial in Stripa in Sweden [6], burial in clay at Mol in Belgium [6,8], in situ testing in limestone in Ballidon in the United Kingdom [6,9], and field testing in salt at the Waste Isolation Pilot Plant (WIPP) in the United States [6,7]. The longest simulated waste glass burial studies (~30 years) are those in the Ballidon limestone as many of the simulated waste glasses were buried in 1978. In the non-radioactive field tests in natural groundwaters, the glasses proved to be as durable and/or more durable than indicated during accelerated laboratory testing [6–9].

Tests have been performed on non-radioactive simulated glasses and/or glasses doped with alpha emitting radionuclides such as ^{134}Cs, ^{90}Sr, and ^{239}Pu. These glasses were subjected to a 5 years burial in the Boom clay at Mol, Belgium at temperatures of 16 °C, 90 °C, and 170 °C for periods of 2–7.5 years. Subsequent experiments were performed with four glasses doped with alpha emitting $^{238-242}PuO_2$, $^{237}NpO_2$, and/or $^{241}Am_2O_3$ [10–13]. These glasses were simultaneously subjected to gamma fields during

---

* Corresponding author. Tel.: +1 803 725 2374; fax: +1 803 725 4704.
E-mail address: carol.jantzen@srnl.doe.gov (C.M. Jantzen).

0022-3115/$ - see front matter © 2008 Published by Elsevier B.V.
doi:10.1016/j.jnucmat.2008.06.040

burial at 90 °C for 5 years. In the case of the alpha emitting radionuclides in the gamma irradiation fields, the durability of the glass was similar to that of accelerated laboratory testing [13].

The leached layers of the glasses buried in Boom clay were examined by scanning electron microscopy coupled with electron diffraction. The SON68 (R7T7) French glass had a leached layer of ~200 μm that was enriched at the top in Al and Si and reduced in Ca and Na. Enrichment in K and Mg was attributed to sorption from the Boom clay. On top of the leached layer were precipitates enriched in Al, Si, Mg, Fe, and K. In-between the leached layer and the precipitates was a region depleted in Si, Al, and Ca. The Belgian glass SM513 (PAMELA) had a 350 μm leached layer enriched in Ti and Al and reduced in Na, Ca, and Mg. Again K was enriched in the layer and attributed to be from the burial medium, the Boom clay. Glass SM527 (PAMELA) had no reaction layer but a thin precipitate layer enriched in K, Mg, Si, and Al. Lastly, Glass WG124 (a silicate glass) had a 500–600 μm layer with a double structure. The outer layer was enriched in Fe, Al, Mg and depleted in Si, Ca, Na, and K while the inner layer was depleted in Mg, Si, Ca, and Na. Precipitates enriched in Si, Al, Mg, Fe, K and S were found on the outermost surface [10].

The Boom clay burial glass with the least reaction layer was the SM527 glass which was the glass highest in Al_2O_3 content, e.g. 19.96 wt% compared to Al_2O_3 contents of 2.9–4.91 for the three other glasses buried. The study concluded that the three lower Al_2O_3 containing glasses dissolved via a combination of network dissolution, selective leaching and ion exchange. The high Al_2O_3 containing glass was determined to leach by a congruent mechanism and only a minor contribution from a selective leaching mechanism.

In some tests the presence of the Boom Clay and ground frit as backfill materials were found to act as silica sources and decrease the glass alteration by two orders of magnitude. The silica rich clay and the silica rich frit provided silica saturated aqueous environments for the glass which inhibited leaching [13]. The glass alteration layer thickness was also found to increase with increasing αβγ-activity of the glass [12].

1.2. Field tests of HLW radioactive glasses

To date there are only two documented HLW glass burial experiments in shallow land disposal sites where lysimeter measurements of radionuclide migration were simultaneously monitored. A third burial study is the focus of this publication.

1.2.1. Chalk river nuclear laboratories (CRNL) field tests

The first and oldest shallow land disposal tests were those at the Chalk River Nuclear Laboratories (CRNL) in Ontario, Canada [14–17]. The waste being immobilized was a HLW UO_2 fuel recycle waste and the major radionuclides were ^{239}Pu and ^{238}U but the activity was primarily generated by ^{137}Cs and ^{90}Sr. Two sets of glass blocks (2 kg each) were buried in a sandy soil aquifer at the CRNL. The glass was made with a glass formers mixture of crushed nepheline syenite rock (51.20 wt% SiO_2, 20.44 wt% Al_2O_3, 4.26 K_2O, 8.53 wt% Na_2O and trace amounts of Fe_2O_3, MgO and TiO_2) and 15 wt% CaO. The blocks were buried without secondary containers, one in 1959 and one in 1960. The compositions of these two sets of glasses were calculated from the data in Ref. [17] and the major components are given in Table 1.

The glasses were exhumed in 1978 and the chemistry and surfaces of the glass and the surrounding soil examined. Laboratory measurements were made on the rates of corrosion of the glass and coupled with field measurements of the rates of ^{137}Cs and ^{90}Sr migration from the glass after shallow burial for ~18–19 years. Measurement of the radionuclides (^{90}Sr and ^{137}Cs) in the surrounding soil indicated that the normalized leaching rates were two orders of magnitude lower than that predicted from the loss of the radionuclides during the laboratory leaching tests [18]. The lower

Table 1

Major components of the tank 15 burial glass in this study compared to other burial glasses

Oxide species (wt%)	SRNL HLW burial glass	SRNL simulated burial glass	SON 68 (R7T7) [12]	SM513 [11]	SM527 (Phase Sep per NAS) [11]	WG124 [11]	Canadian HLW burial test #1 [17]	Canadian HLW burial test #2 [17]	Russian LAW K26 [24,25,77]
Waste loading (wt% calcine oxide)	~31[c]	~31[c]	UNK	UNK	UNK	UNK	1.5	8	35
Radioactivity[d]	500 MBq/g(β/γ)	N/A	(up to 1GBq/g α when doped with Am_2O_3)[a]	UNK	UNK	UNK	~420 MBq/g(β/γ)	~1400 MBq/g(β/γ)	3.8E–03 MBq/g(β/γ)
Al_2O_3	6.67	6.99	4.91	3.59[b]	19.96	2.9[b]	20.44	19.37	3.1[b]
B_2O_3	7.54	7.57	14.02	13.08	21.70				6.6
CaO	4.16	5.18	4.04	4.54	3.87	4.1	15.00	13.80	13.7
Cr_2O_3	0.50	0.47	0.51	0.27	0.02	2.2		0.18	
Fe_2O_3	10.08	9.94	2.91	1.67	0.7	12.5	0.06	2.30	1.7
Li_2O	3.02	3.11	1.98	4.18	3.10				
MgO	0.23	0.23		2.05	0.14	2.9	0.02	0.22	
MnO	1.79	1.74		0.53	0.02				0.95
Na_2O	13.74	14.83	9.86	9.05	7.77	3.6	8.53	11.39	23.9
NiO	0.82	0.69	0.41	0.42		1.1		0.20	
SiO_2	45.78	44.93	45.48	52.15	38.75	60.7	51.2	47.10	43.00
SrO	0.74		0.33	0.045			0.023	0.006	
ThO_2	0.11		0.33						
UO_2	2.43	2.67	0.52	0.104	0.02			0.96	
ZnO	0.02	<0.01	2.50	0.016					
ZrO_2	0.04	0.04	2.65	0.79	0.05				

[a] The SON68 glass buried was doped with 1 GBq/g α (Am_2O_3) while COGEMA plant active glasses are ~10 GBq/g β/γ [78].

[b] During development of THERMO™ it was determined that a minimum of 4 wt% Al_2O_3 was necessary in high Fe_2O_3 containing and high Na_2O containing glasses to avoid phase separation [79] unless sufficient ZrO_2 was present as well. This is consistent with the known miscibility gap in the Al_2O_3–Fe_2O_3–Na_2O–SiO_2 quaternary system (no ZrO_2) that defines the crystallization of basalt [80]. The HLW waste glasses with <4.0 wt% Al_2O_3 were subject to poor durability due to the phase separation. Confirmation is also provided by commercial glasses in the Na_2O–SiO_2–Al_2O_3 system which are known to phase separate when Al_2O_3 is ⩽3 wt% [81,82].

[c] Calculated from the B_2O_3 and Li_2O compositions measured in the burial glass in this study once normalized to 100 wt% and the Frit 211 composition given in Section 3.1 normalized to 100 wt%.

[d] where MBq (megabecquerel, 106 Bq) and GBq (gigabecquerel, 108 Bq).

leach rates from the field study were attributed to the lower temperature in the field tests compared to the laboratory tests. Ref. [17] states that the neither the laboratory nor the field leach rate measurements indicate congruent or diffusion-controlled dissolution mechanisms for the glass. The leach rate time dependence, inferred from the ^{90}Sr ground-water concentrations, suggests that the dissolution is being inhibited by a surface layer [16]. In addition, the ^{90}Sr was found to have sorbed onto iron oxyhydroxides in the surrounding soil so that migration of this radionuclide was retarded.

Depth profiling of the glass block surface with Secondary Ion Mass Spectroscopy (SIMS) showed that Ca, Na, Cr, and Fe were depleted down to a depth of 70–80 nm (0.07–0.08 μm) of the surface while Si, Mg, and Th were enriched in the surface layers [17]. Thorium was enriched to a depth of ~100 nm (0.1 μm) as was U but Fe and Mg were only enriched to a depth of ~45 nm (0.045 μm). Since the glass contained little Mg, the Mg enrichment was thought to be a magnesium silicate that had formed from the silica in the glass and the Mg in the groundwater. The thickness of the material removed during the ~20 years burial test was estimated from the Th enrichment and corresponded to a 400 nm (0.4 μm) loss from the original glass surface. The leached layer was found to contain a 'fixed' ferromagnesian fraction which sorbed 13–14% of the ^{90}Sr [16].

1.2.2. Nuclear power plant (NPP) intermediate level waste field tests

In 1987 blocks of K26 glass used to immobilize intermediate level nuclear power plant (NPP) waste from the Kursk (RBMK) reactor in Russia were buried in a loamy soil [19]. The glass was poured into carbon steel rectangular containers that did not have lids. The glass containers without lids were buried in a steel tray that was supplied with a water trap and a tube for water extraction by pumping. The tray was deeper than the pour containers and the tray was filled with pure sand before the rest of the burial trench was backfilled with the loamy soil [20]. While the conditions are considered saturated the glass was not in direct contact with the loamy soil.

Waste glass with 35 wt% waste oxides was produced [21]. The K26 glass is a high sodium containing borosilicate glass made from a waste containing 86 wt% $NaNO_3$ [19,21] and the prime contaminants were ^{137}Cs (82%), ^{134}Cs, and ^{90}Sr. Both saturated groundwater and non saturated groundwater conditions were studied [22,23]. The blocks buried under unsaturated conditions were examined after 8 years burial [24] and the leached layer was determined to be 2–6 μm by scanning electron microscopy (SEM). The blocks buried under saturated conditions were extensively studied after 12 years of burial [22,25]. In 2001, X-ray analysis and SEM of the surface of the glass buried under saturated conditions showed no evidence for the formation of secondary alteration phases on the glass surface [22]. Re-analysis in 2004 [25] identified some small crystalline inclusions of quartz (SiO_2), calcite ($CaCO_3$), hematite (Fe_2O_3) and anatase/rutile (TiO_2) although the layer was primarily amorphous. About 1.3E-03 percent of the radioactivity had leached into the groundwater during the 12 year period, mainly ^{137}Cs.

1.2.3. Savannah River national laboratory (SRNL) field tests

Details of the third HLW glass burial are given in this study. A radioactive Savannah River Site (SRS) HLW waste glass was buried in a lysimeter located ~11 m above the water table. As such the glass was exposed to saturated and unsaturated conditions as controlled by local rainfall and weather conditions. The glass was left in the field lysimeter for 24 years before it was recovered by coring. The lysimeter was open for 11 years and capped for 13 years. The bulk glass composition was analyzed after the glass was exhumed. The formation of a leached layer and the glass/soil contact zone was studied by scanning electron microscopy (SEM).

The SRS burial glass composition was used to assess the glass durability in two ways. First, the glass composition was analyzed and the composition used to predict the glass durability using the SRS model that has been used to operate the SRS vitrification facility for ~15 years (the Thermodynamic Hydration Energy Model, THERMO™) [26–28]. The THERMO™ model is based on a short term accelerated 7-day durability test, ASTM C1285 [29]. The durability of the burial glass was measured using the same accelerated glass durability test. The short term durability of the burial glass was then related to the long term durability with respect to the leached layer using the recently developed Activated Complex Theory (ACT™) [30] and the glass composition.

2. Stages of glass dissolution

Current theories of glass dissolution suggest that all glasses typically undergo an initial rapid rate of dissolution known as the 'forward rate'. However, as the contact time between the glass and the leachant lengthens some glasses come to 'steady state' equilibrium and leach at a 'steady state' rate while other glasses undergo a disequilibrium reaction with the leachant solution that causes a sudden change in the solution pH or the silica activity in solution [1]. The 'return to the forward rate' after achieving 'steady state' dissolution is undesirable as it causes the glass to return to the rapid dissolution characteristic of initial dissolution.

The initial rate is often referred to as Stage I dissolution which includes regimes that are interdiffusion controlled, hydrolysis controlled, and a rate drop that is diffusion or affinity controlled [31]. The 'steady state' rate (also known as the residual or final rate) which signals the end of the alteration phase and/or phase precipitation [31] is known as Stage II dissolution, and the return to the forward rate (or resumption of alteration) is known as Stage III dissolution. Diffusion controlled dissolution of network modifiers and/or radionuclides during Stages I and II dissolution normally follow a mathematical function related to the square root of the test duration.

A reaction zone is formed as the leached layer solution interface progresses into the glass. The front of the reaction zone is usually defined as the region where the glass surface sites interact with the ions in solution [32]. The top of the gel reaction zone represents the leached layer glass interface where a counter-ion exchange occurs [32] that can form secondary precipitates, e.g. metal hydroxo and/or metal silicate complexes that have reached saturation in the leachate often precipitate on the surface of the gel layer [33–38]. The gel layer may, under certain conditions, act a selective membrane [35,39] or as a protective/passivating layer [33,34,37,38,40–44]. The slowing of the glass dissolution to a steady state rate by solution saturation (affinity) of glass matrix elements or reaction through a surface layer is referred to as Stage II dissolution, residual rate dissolution, steady state dissolution, or the final dissolution rate. The leached layer is often a simple Fe^{+3}-rich phase such as the clay mineral nontronite (see Section 2.1).

The resumption of alteration (Stage III) causes the long term dissolution rate to reaccelerate at the initial forward dissolution rate for some glasses. This unexpected, and poorly understood, return to the forward dissolution rate has been shown to be related to the formation of the Al^{3+}-rich zeolite, analcime, and/or other calcium silicate phases [1].

2.1. Aging of HLW glass gel layers: why the Al^{3+} and Fe^{3+} content of the gel layer is important

Experimental aging of the hydrated gel layers formed during Stage II glass dissolution has shown that the gel layer components age in situ into either clay mineral assemblages or zeolite mineral assemblages [43,45–48]. Many of the burial studies cited in the introduction have examined the glass leached surface layers and/or the glass/soil interface which includes the leached layer reaction zone. The results are often conflicting, e.g. the Belgian study found the leached layers to be preferentially enriched in Al^{3+} over Fe^{3+} or both Al^{3+} and Fe^{3+}. The Russian and Canadian studies found the leached layer to be enriched in Fe^{3+} preferentially and in the Canadian burial study ^{90}Sr appeared to be sorbed onto the ferromagnesian fraction of the leached layer. Since the glass leached layer/soil interface is often the primary focus of a burial test, it is important to understand how the burial conditions and glass chemistry can impact the observations. In addition, Al^{3+} is normally in tetrahedral coordination in HLW glasses and is thus a matrix or structural element like Si^{4+} that can contribute to both the affinity term and the leached layer formation. In defense waste glasses, that are deficient in Al^{3+}, the Fe^{3+} is normally in tetrahedral coordination as well and can contribute to both the affinity term and the leached layer formation.

In order to understand the aging of a leached glass gel layer into either clay or zeolite mineral assemblages, it is important to recognize that the hydrated gel layer exhibits acid/base properties which are manifested as the pH dependence of the thickness and nature of the gel layer [49]. The alteration of aluminosilicate gels (artificial or natural) to clay or zeolites is pH dependent, with clay formation favoring less basic aging environments than zeolites [50]. Thus, if the solution pH changes while the gel ages (as in a static laboratory test) a clay mineral species may convert into a zeolite mineral species in response to an increase in pH.

The in situ aging of aluminosilicate rich leached layers in HLW glasses mimics the aging of pure aluminosilicate gels: artificially produced gels and those found in nature. Aluminosilicate gels that were co-precipitated under controlled laboratory conditions were aged into a variety of natural clays (smectities, beidellites, saponites, sauconites and montmorillonites) [51–53]. Aluminosilicate gels found in natural geothermal systems in an alkaline environment were harvested and then aged in the laboratory to the zeolite analcime [54]. The alteration of aluminosilicate gels (artificial or natural) to clay or zeolites is pH dependent, with clay formation favoring less basic aging environments than zeolites [50]. Aging of leached gel layers in natural environments, e.g. weathering of altered rhyolitic (acidic) volcanic glass, has been shown to alter in situ to both zeolites (clinoptilolite) and clays (smectitie, montmorillonite), and sometimes opal (hydrous silica) [54–56].

Conversely, sequential aging of nuclear waste glass gel layers that were enriched in iron under controlled laboratory conditions produced montmorillonite clay [57] and the in situ formation of smectite clays has been determined to be dependent on the iron content of the dissolving glass [58]. The similarity of the gel layer formation and dissolution mechanism of iron containing borosilicate waste glasses and natural basalt glasses containing iron has been noted by several researchers, i.e. Morgenstein and Shettel [59], Ewing [60], Malow et al. [61], Allen [62], and Jantzen and Plodinec [63]. In particular, the work of Allen [62] indicated that the alteration layer on basalt glass is formed of cryptocrystalline iron rich clays grouped under the term 'palagonite'. Likewise, the geochemical modeling (EQ3/EQ6) performed by Bourcier et al. [64] on an iron rich waste glass gel layer composition predicted the formation of notronite ($Fe_2Si_2O_7 \cdot 2H_2O$) the iron analogue of the Al-rich clay mineral kaolinite ($Al_2Si_2O_7 \cdot 2H_2O$). Additional comparisons of the aging sequences of basaltic glasses and nuclear waste glasses tested using the Vapor Hydration Test (VHT) have demonstrated that clays can only turn into zeolites as the solution becomes more basic and more saturated with silica and alumina during static durability testing [47,48].

Moreover, the role of Al^{3+} and Fe^{3+} in the HLW glass, in the leached layer, and in the leachant has been shown to be involved in whether a glass maintains Stage II 'steady state' dissolution or reverts to the forward rate of dissolution, e.g. Stage III dissolution. Van Iseghem and Grambow [1] demonstrated that an Al^{3+}-rich zeolite (analcime) formed on certain glasses during dissolution but not on others. The formation of analcime in these experiments carried out at 90 °C at SA/V conditions of 10, 100, and 7800 m^{-1} accelerated the glass corrosion by consuming H_4SiO_4 from the leachate solution but did not accelerate the glass corrosion back to the original forward rate, e.g. 'the formation rate of analcime is too small to bring the glass dissolution rate back to the forward rate' [1]. Two different glasses were studied, SM58 which contained 1.2 wt% Al_2O_3 and 1.2 wt% Fe_2O_3 and SAN60 which contained 18.1 wt% Al_2O_3 and 0.3 wt% Fe_2O_3. The SAN60 glass with the highest concentrations of Al_2O_3 and the lowest amount of Fe_2O_3 was the glass that formed the analcime reaction product. These authors also demonstrated that a change in solution pH accompanied the return to the forward rate when analcime formed. Likewise, Inagaki et al. [65] demonstrated that solution pH and solution concentrations of Na and K were also involved in the formation of analcime versus Na-bedellite (a smectite clay). Other zeolites and smectite clays that are rich in Fe^{3+} compared to Al^{3+} do not appear to accelerate glass corrosion [1,3].

Thus, research has shown [66] that different pH values are achieved during static testing at different SA/V ratios and that affects the reaction rate and the phases that form. This is important when studying or comparing the results of accelerated laboratory tests to burial tests: are the SA/V•t conditions equivalent, is the alteration extent equivalent, and is the corrosion mechanism the same even if the SA/V•t is different [66]?

For the burial studies examined to date (Sections 1.2.1 and 1.2.2), the leached layers have generally been found to be enriched in Fe^{+3}-rich phase such as the clay mineral nontronite or an Mg-Fe phase where the Mg component was supplied from the surrounding clay. For example, (1) the 'ferromagnesian' rich leached layers observed in the CRNL field burial tests [16], (2) the Fe_2O_3-rich hematite mineral phases found on the Russian K26 burial glass [25], and (3) the notronites predicted by EQ3/EQ6 geochemical code from the Russian K26 burial glass leached layer compositions [21,67].

3. Experimental

As a part of a radionuclide migration research program, SRNL initiated a lysimeter project in 1978 to study the migration of low-level transuranic (TRU) contaminates from various waste forms buried under actual field conditions. One HLW glass cylinder (1.3 cm in diameter and 1.3 cm in length), representative of glass compositions currently being processed at the Defense Waste Processing Facility (DWPF), was buried in 1981. The glass was exposed to natural rainfall in the unsaturated zone for 11 years. Occasionally, during periods of heavy rainfall (>4 per month) the groundwater table would rise and the soil inside the lysimeter would become saturated. The lysimeter leachates were only sampled for the first 8 years of exposure.

3.1. Fabrication of the HLW glass

Defense HLW was once an acid waste that was neutralized for storage in carbon steel tanks. The neutralization caused the waste to settle into a thick sludge component and a low density salt supernates. The glass was made with Tank 15 waste which is a high alumina containing HLW waste sludge. The alumina is present as $Al(OH)_3$, AlOOH, $Al(OH)_4^-$, and other soluble aluminum salts. The high aluminum content is detrimental to making a quality vitrified product at reasonable waste loadings [68].

A large sample of Tank 15 waste had been retrieved from the tank in 1978. Several aluminum removal processes were tested in the SRNL Shielded Cell Facility to remove the soluble alumina in water and/or excess NaOH [68]. One test was performed in water only, two tests were performed in boiling 5 molar NaOH, and the fourth test was performed with 3 molar NaOH. The caustic treated sludges were mixed with water and centrifuged several times to 'wash' the soluble salts out of the sludge in order to make a durable glass with a soluble salt level <2 wt% on a dry basis. The alumina containing liquors can then be stabilized in cement.

At the end of the various Al dissolution and 'washing' demonstrations the three caustic washed sludges were blended back together and reslurried with water [68]. The sludge slurry was fed to a fluid-bed calciner with a bed temperature of 350 °C. The washed and dried Tank 15 sludge was mixed with Frit 211 (SiO_2 = 58.3, B_2O_3 = 11.1, Na_2O = 20.6, Li_2O = 4.4, and CaO = 5.6) in a weight ratio of 35/65 dried waste/sludge which is ~28 wt% waste loading when all of the remaining insoluble nitrates, oxalates, and sulfates are destroyed at temperatures between the drying temperature of 350 °C and the vitrification temperature of 1150 °C.

The glass was processed through a Joule heated melter in the Shielded Cell Facility in SRNL at a temperature of 1150 °C. Most of the glass was collected in 500 mL stainless steel beakers. At the end of two of the melt campaigns, glass samples were poured into small graphite molds and archived for leaching experiments. The filled glass canisters and the graphite molds were allowed to cool in a brick fort beside the melter to simulate the slow cooling of a DWPF type canister. The glass was not analyzed at the time it was made. One of the small graphite mold samples was the burial glass examined in this study.

The radionuclide concentrations in the glass were calculated from the radionuclides measured in the sludge as given in Ref. [68] accounting for the sludge density, sludge washing percent, the calcine oxide factor, the waste loading, and the weight of the glass pellet. The radionuclide loading in the glass pellet at the time of burial is given by the values in Table 2. The primary radioactivity in the Tank 15 glass was ^{90}Sr and its radioactive daughter ^{90}Y. The table also includes other short lived radionuclides that are daughters of the radionuclides measured. Clearly the main type of radiation from the glass is beta radiation.

3.2. Burial and retrieval of the HLW glass

The lysimeter consisted of an inverted 52-L bottomless carboy that was connected to a leachate collection reservoir (Fig. 1). The lysimeter was filled with well-mixed subsurface sediment collected from a 4-m-deep pit from which the surface soil had been removed. The sediment used in this study was primarily collected from the vadose zone and contained no observable biological materials. The sediment had a pH of 6.3, total Fe concentration of 1.6 wt%, along with sand, silt and clay with concentrations of 71, 10, and 19 wt%, respectively. The clay-fraction consisted of kaolinite, hematite, goethite, gibbsite, and quartz.

Table 2
Radionculide content, including principal radioactive daughters, of the initial glass monolith (from Ref. [70])

Radionuclide	Half life (years)	mCi/4.75 g	Principal mode of decay
^{90}Sr	28.8	31.68	β
^{90}Y	7.3E–03	31.68	β
^{144}Ce	0.787	0.12	β
^{144}Pr	3.3E–05	0.12	β
^{137}Cs	30.1	0.11	β
^{137m}Ba	4.9E–06	0.10	γ
^{60}Co	5.3	0.11	β
^{154}Eu	8.6	0.08	β
^{106}Ru	1.0	0.02	β
^{125}Sb	2.8	0.02	β
^{238}Pu	87.7	0.03	α
^{239}Pu	2.4E–04	<0.01	α

The glass pellet (described in Section 3.3) was placed ~21.6 cm below the lysimeter sediment surface on the centerline of the carboy in lysimeter M2 (Fig. 1). The lysimeter was left exposed to natural weather conditions for 11 years before being capped for an additional 13 years. A soil core was taken after the lysimeter had been capped for 5 years. This was 16 years after emplacement of the glass. The core was stored in a cooler at 16 °C for 9 years before analysis. The glass remained in the lysimeter for a total of 24 years before it was recovered. During recovery it was observed that the glass had been fractured apparently during the soil core sampling, the placement of the cement cap, or the recovery operation itself. A picture of the largest fraction recovered is shown in Fig. 2.

During the first 8 years of the 11 years that the lysimeter was open, leachate from the lysimeter was periodically sampled (May 1981–December 1989) and analyzed for gross α and gross β/γ. Samples were taken monthly from 1981 until June 1983 when the sampling frequency was changed to quarterly. After 1987 the sampling frequency was irregular and sometimes ~6 months. The data from this final time period are erratic and not used in this study. The alpha and beta/gamma was measured with a Baird Instruments detector attached to a Scintillation Counter. A control lysimeter (M11) was also monitored for gross α and gross β/γ. Most of the alpha counts in leachates from in the control lysimeter were slightly higher than the counts in the glass lysimeter. This is likely because the alpha emitters (^{238}Pu, ^{239}Pu, and ^{240}Pu) in the glass pellet are of very low concentrations in the glass (Table 2) compared to the beta emitters (primarily ^{90}Sr and its radioactive daughter ^{90}Y). Since the alpha data collected were usually below the alpha data from the percolate from the control lysimeter, the alpha data was not used in the durability modeling presented in a subsequent section. The β/γ data that was below the counts for control lysimeter was also not used in modeling.

The lysimeter soil core taken 16 years after emplacement of the glass was cut into twenty two 1.25–2.5 cm thick slices. These depth discrete sediment samples were acid digested and then analyzed for total α (^{238}Pu, ^{239}Pu, and ^{240}Pu) and total β by liquid scintillation counting. They were also analyzed for ^{137}Cs by gamma pulse height analysis, respectively. As discussed above, the glass pellet was exposed to natural climatic conditions for ~11 years and was in contact with moist soil for a total of 24 years.

3.3. Characterization of the HLW glass

After the Tank 15 glass was unburied the following analyses were performed:

- Contained X-ray diffraction (CXRD) of the glass surface.
- – Analysis performed on a Bruker D8 advanced X-ray diffractometer with Cu Kα radiation at 45 kV and 40 mA.
- Contained scanning electron microscopy (CSEM) of the glass/soil layer interface.
- – Analyses performed on a LEO-440 scanning electron microscope. The energy dispersive spectra (EDS) were acquired using an Oxford Inca microanalysis system.
- – The sample was embedded in epoxy and sectioned perpendicular to the glass/soil interface.
- Whole element chemistry of the bulk glass by
- – Dissolution by Na_2O_2 with an HCl uptake followed by inductively coupled plasma (ICP) – emission spectroscopy (ES) for Al, B, Ba, Ca, Ce, Cr, Cu, Fe, La, Li, Mg, Mn, Mo, Ni, Si, Sn, Sr, Ti, and U and ICP-mass spectroscopy (MS) for Th.
- – Dissolution by HCl/HF bomb followed by ICP-ES for Na, Zn, and Zr.

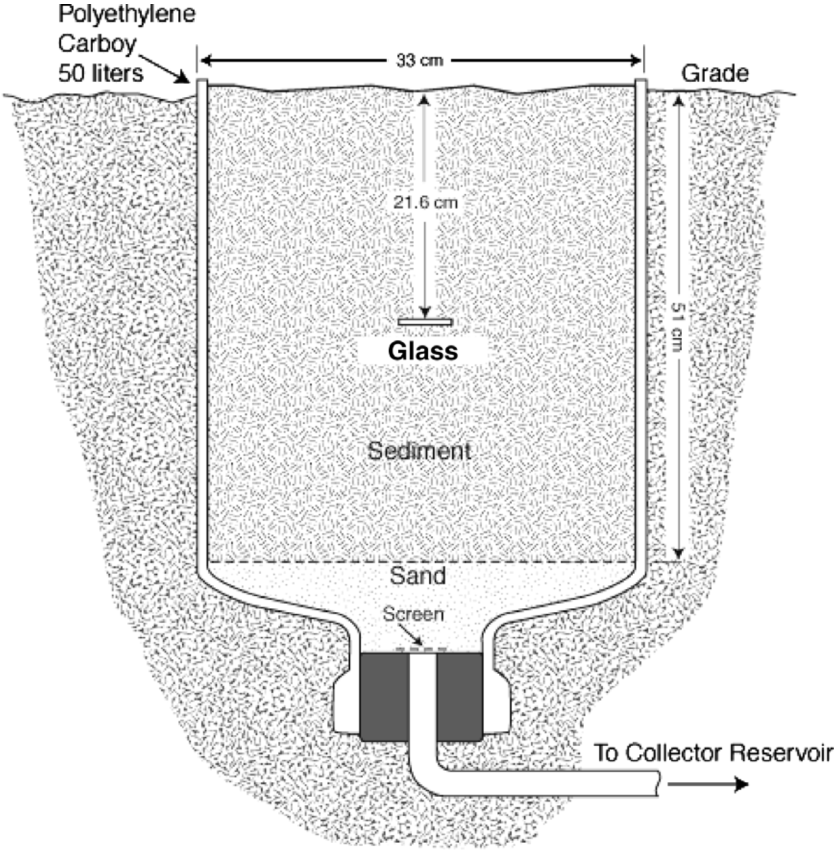

Fig. 1. Schematic of the Tank 15 HLW glass burial lysimeter.

Fig. 2. Burial glass fragment exhumed after 24 years (a copper penny for scale).

Anions were not measured as the anion content of the glass was predicted to be very low from analysis of the Tank 15 sludge [68] and analysis of the washed/dried sludge [69]. Glasses were analyzed in duplicate and both the Environmental Assessment (EA) glass [70,71] and the ARG-1 glass [72] were used as glass standards.

3.4. Durability testing of the HLW glass

There was not enough of the Tank 15 burial glass left to perform triplicate ASTM C1285 (Product Consistency or PCT) durability testing. A glass of the same composition was fabricated in crucibles and rapidly quenched. This glass was analyzed as shown in Section 3.3 and tested via ASTM C1285 (PCT-A). The results of the PCT test are expressed in this study as a normalized concentration (NC_i) which has the units of $g_{\text{waste form}}/L_{\text{leachant}}$, where '$i$' is the chemical element of interest. Expression of the PCT test response as NC_i does not necessitate the use of the surface area (SA) of the sample releasing species 'i' as the surface area is fixed by the strict control of the particle size during the PCT-A test[1] and the control of the volume of the leachant being used which is expressed as the SA/V ratio

$$NC_i = \frac{c_i(\text{sample})}{f_i}, \tag{1}$$

where NC_i is the normalized release ($g_{\text{waste form}}/L_{\text{leachate}}$), c_i (sample) is the concentration of element i in the leachate solution (g_i/L) and f_i is the fraction of element i in the unleached waste form (unitless).

4. Results and discussion

4.1. Analysis of the disposal environment and lysimeters

A photograph of a recovered glass fragment is presented in Fig. 2. The crusty material on the black glass is the soil and extreme

---

[1] The glasses were ground and sized between −100 and +200 mesh (74–149 μm). To remove the electrostatic fines, the sized material was washed six times with 100% ethanol. Water was not used for washing for fear of removing any water soluble phases prior to leaching as cautioned by the ASTM C1285-02 procedure. For all samples, ASTM Type I water was used as the leachant, a constant leachant to sample ratio of 10 cm^3/g or 0.01 L/g was used, the test temperature was 90 °C. The test duration was seven days. The test temperature and duration are the nominal test conditions used for testing glass waste form performance, e.g. PCT-A. Stainless steel vessels were used.

care was taken to ensure that the soil/glass interface was retained for study. The entire glass cylinder could be reconstructed from the fragments collected in the sediment.

The cumulative alpha activity of leachates from the glass lysimeter was less than or equal to that for a control lysimeter. This indicates that the alpha emitting radionuclides ^{238}Pu, ^{239}Pu, and ^{240}Pu if they leached from the glass did not leave the lysimeter with the leachates.

Radionuclide profiling for total alpha, ^{137}Cs, and total beta activity in the single core sample indicated that the radionuclides ^{238}Pu, ^{239}Pu, and ^{240}Pu were not enriched in the soil in the core removed from the lysimeter while the ^{137}Cs and beta activity (primarily ^{90}Sr, ^{90}Y, and ^{137}Cs) were enriched in the first few centimeters of soil near the glass pellet (Fig. 3). In Fig. 3, positive distances from the source were above the source and negative distances were below the source. The type of profiles observed for the ^{137}Cs and the total beta are expected based on a diffusive mechanism for migration of the radionuclides in the soil. Also based on the data in Fig. 3(a) and (c), it appears the ^{90}Sr diffused further from the source than the ^{137}Cs. This could be due to the higher concentration of ^{90}Sr in the glass pellet or stronger sorption on the soil. Based on the low beta/gamma activity measured in the leachates, the ^{137}Cs and ^{90}Sr that was leached from the glass appeared to be sorbed by the sediment, perhaps by the iron oxyhydroxides in the soil as observed in the CRNL study [17]. Finally there is evidence that the Pu isotopes leach from the glass slower than ^{90}Sr and ^{137}Cs [73]. This could also account for Pu not being detected in the sediment of the core samples (Fig. 3(a)).

4.2. Analysis of the HLW glass

4.2.1. Chemical analysis and comparison to other burial glasses

The analyses performed on the burial glass are described in Section 3.3. The burial glass and the standards were dissolved in duplicate and each analyte was analyzed once. The non-radioactive standards were analyzed simultaneously and handled in the same manner as the burial glass. The replicate analyses of the burial glass and the standards were averaged. The responses for several elements in the standards were biased either high (Ca, Fe, and Mn) or low (Al, B, and Na,). Glass compositions were bias corrected to the standard glasses for all elements that were in error by $\geqslant$4%. The overall composition of the glass is given in Table 1. The calculated waste loading based on the B and Li content of the frit added was calculated to be $\sim$31 wt%. The SRNL glass radioactivity was calculated to be $\sim$500 MBq/gβ/γ.

The SRNL burial glass composition, waste loading, and radioactivity are compared to those of the CRNL burial glass, the Belgian doped glass burial studies, and the Russian K26 glass. The SRNL burial glass waste loading was high and the total β/γ radioactivity (500 MBq/g) was about the same value as the first CRNL burial glass (420 MBq/g) but lower than the second CRNL burial glass. The SRNL glass was higher in β/γ radioactivity than the Russian glass which had a β/γ of 3.8 E-03 MBq/g. The SRNL glass was much lower in radioactivity than the doped Belgium burial glass SON68 glass of which contained about $\sim$1 GBq/g α from Am_2O_3 (Table 2).

4.2.2. Scanning electron microscopy and X-ray diffraction

The X-ray diffraction (XRD) of the SRNL burial glass surfaces was performed on four different samples. The primary phases were kaolinite clay from the surrounding soil and quartz (SiO_2). In two of the four samples gibbsite ($Al(OH)_3$) and/or boehmite (AlOOH) were indicated as minor probable phases. Any other components were either below detection limit or amorphous.

Scanning electron microscopy with backscatter elemental mapping was performed of the glass/soil interface. A very thin leached layer that ranged in thickness from <8 μm to 8 μm with occasional regions as thick as 32 μm were observed (Fig. 4). The leached layer of the SRNL burial glass is much smaller than the 200–350 μm leached layers observed in the Belgium doped burial studies at 90 °C. This is to be expected as the SRNL study was conducted at ambient temperatures. In both studies the glass was buried in a clay rich soil but the Boom clay is rich in humic acids which promote colloidal transport [74] while the SRS Fe_2O_3-rich clay is oxidizing.

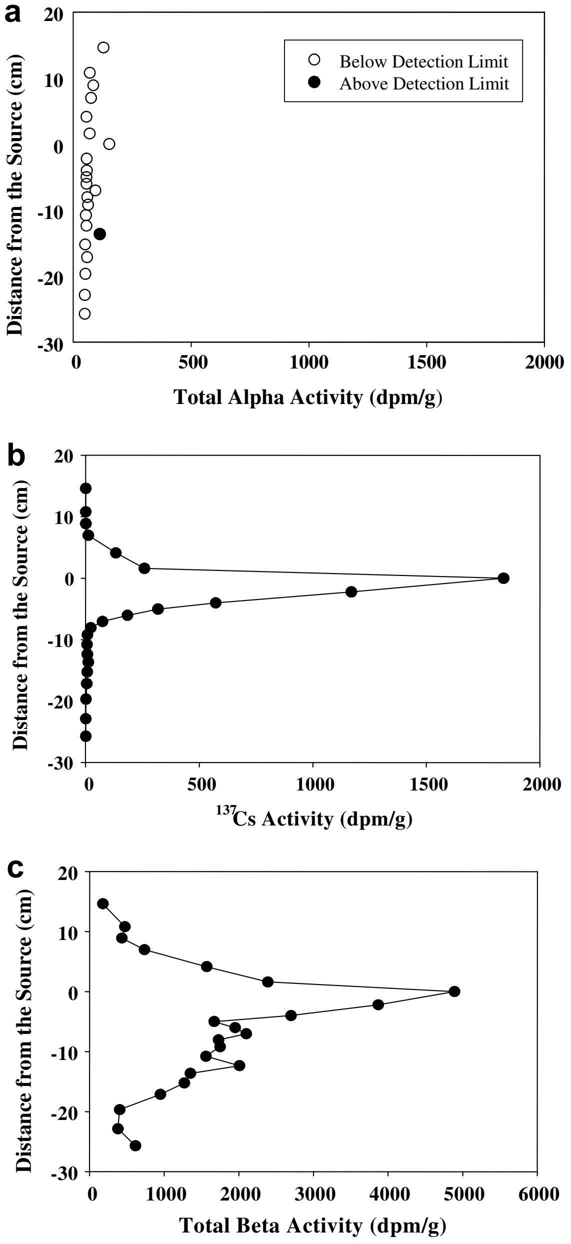

Fig. 3. Radionuclide and activity distribution in sediment around buried glass pellet.

The SRNL burial glass leached layers are somewhat thicker ($\sim$10X) than the CRNL nepheline syenite glass leached layers. This is also expected as boron free, nepheline syenite glass is more durable than lower temperature borosilicate type glasses. In addition, the SRNL glass was buried for 5 years longer than the CRNL glass. The SRNL burial glass leached layer is about the same order of magnitude as the Russian K26 glass leached layer indicating that 2–8 μm may be typical of borosilicate glasses buried at ambient conditions for 12–25 years.

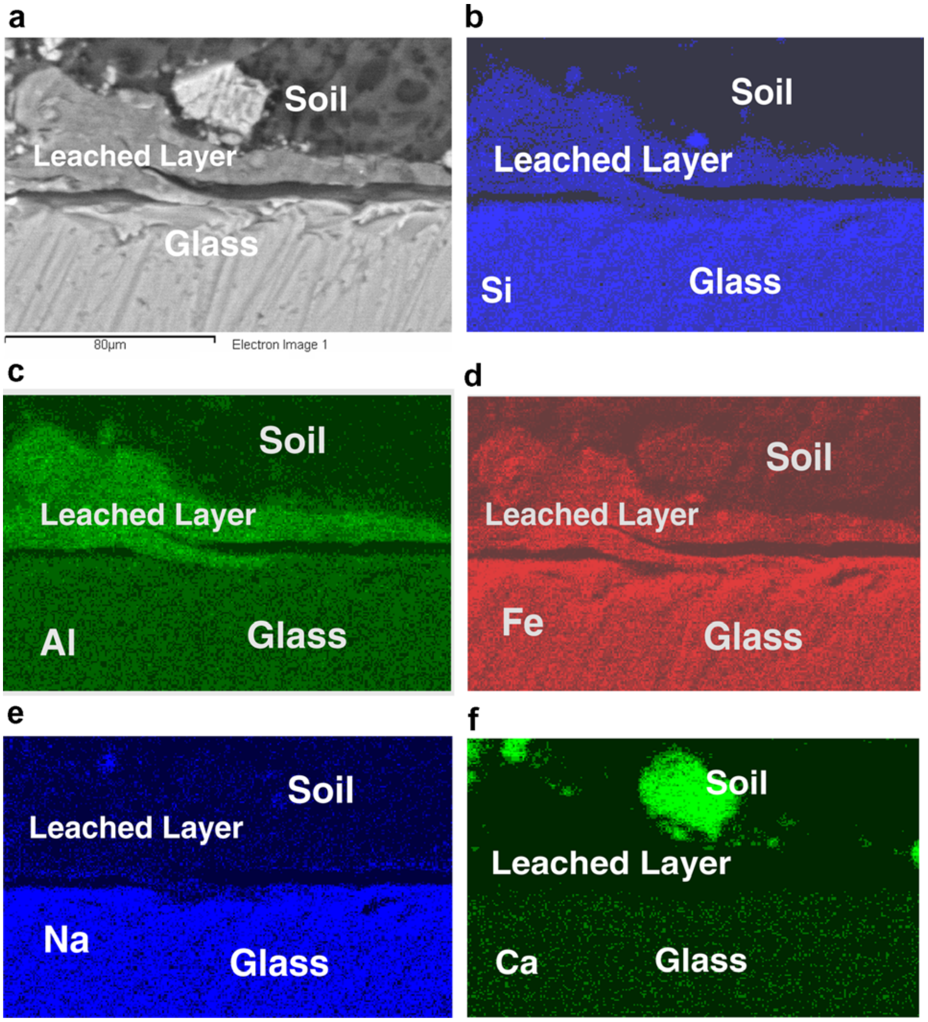

Fig. 4. Energy Dispersive Spectra for soluble species such as K, Na, Ca and insoluble species that participate in the leached layer formation (Si, Al, and Fe) and insoluble species that remain in the glass (Mn). Note the nodule of a Ca-rich species in the soil, likely $CaCO_3$.

The SEM/EDAX elemental mapping of the glass/soil interface (Fig. 4) demonstrates that the leached layer is enriched in Si, Al, and Fe while depleted in Na, Ca, and Mn. There are isolated nodules of a Ca-rich phase in the soil that may be $CaCO_3$ as observed in the K26 glass leached layers. The enrichment of Al, Fe, and Si was also noted in the CRNL and Belgium burial studies.

The SEM/EDAX elemental mapping of the glass/soil interface (Fig. 4) also indicates that the Tank 15 burial glass has a simple leached layer depleted in alkali and alkaline earths but enriched in Al, Fe, and Si. These are the types of leached layers typically observed on simulated SRNL HLW glasses [35] designated as Type II leached layers by Hench and Clark [40] by infrared (IR) studies of glass surface bonding (Si–O–Si) and secondary ion mass spectroscopy (SIMS).

4.3. Durability testing of the HLW glass

A simulated Tank 15 glass was made for durability testing since the amount of burial glass was insufficient for triplicate durability analyses by ASTM C1285 (Product Consistency Test, PCT). The simulated glass was analyzed by the same methods as used on the burial glass (Section 3.3) and the analysis is given in Table 1 and shown to be very similar to the composition of the burial glass. The ASTM C1285 leachate data was calculated using (Eq. (1)) and the results are given in Table 3. Two standards, the Approved Reference Material (ARM-1) and the Environmental Assessment (EA) glass were run as internal standards during the leaching experiment. The analysis of the standards from this study is given in Table 3 and the results are compared to round robin results for each of these standard glasses. The test results on the standard glasses, which achieved the standard round robin response, demonstrate that the Tank 15 glass durability tests were in control.

4.4. Comparison of measured durability to predicted glass durability

It is of interest to compare the predicted durability of the Tank 15 glass from the durability model THERMO™ [26,27] to the measured durability in the accelerated short term (7 day) ASTM C1285 (PCT) test. The ASTM C1285 test results are given in Table 3 in terms of NC_i (Eq. (1)) in g/L and shown graphically in Fig. 5 plotted against the composition term, the preliminary free energy of hydration. The measured Tank 15 glass durability from the short term laboratory testing agrees well with the THERMO™ model prediction.

4.5. Diffusion controlled leaching behavior

The rainfall, total alpha in pCi/mL, and total beta/gamma in pCi/mL in the lysimeter was measured from May 1981 to November 1989 (Fig. 6 top). The rainfall data was converted to an effluent vol-

Table 3
Product consistency test (ASTM C1285) results for the Tank 15 simulated glass and standards used during testing

	ARM standard (this study)	ARM (published round robin) [74]	EA standard (this study)	EA (published round robin) [72,73]	Tank 15 HLW glass (this study)
Log $NC_{(B)}$ g/L	−0.28	−0.29	1.29	1.22	−0.06
Log $NC_{(Li)}$ g/L	−0.23	−0.24	1.00	0.98	−0.08
Log $NC_{(Na)}$ g/L	−0.30	−0.30	1.16	1.13	−0.06
Log $NC_{(Si)}$ g/L	−0.55	−0.55	0.62	0.59	−0.36

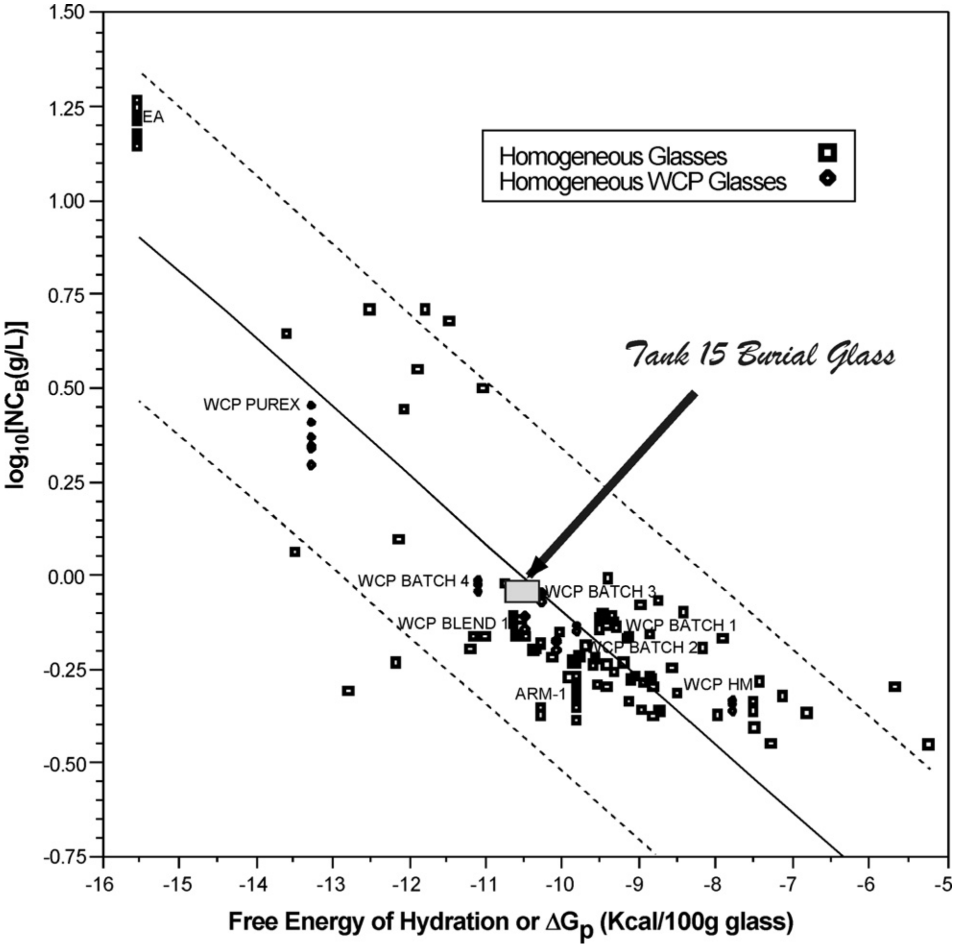

Fig. 5. Performance of the SRNL Tank 15 burial glasses as measured by the short-term (7-day) Product Consistency Test and the THERMO™ model based on boron releases. (NC_B is the Normalized Release ($g_{\text{waste form}}/L_{\text{leachate}}$) as defined in **Eq.** (1).) The Waste Compliance Plan (WCP) glasses shown on the Fig. are reference glasses that bracket the composition of the glasses intended to be processed in the SRS HLW melter.

ume assuming a standard 0.66% evapo-trasporation factor due to the warm climate in South Carolina all year long. Since the evapo-trasporation factor is a constant it does not affect the discussion the diffusion controlled leaching mechanism. The time dependence of the groundwater volume and the specific radioactivity of the groundwater that contacted the waste glass (Fig. 6 bottom) followed a square root dependency with time.

The groundwater concentration data (pCi/mL) measured with the Baird Scintillation Counter were converted to Bq/L to be consistent with the dissolution modeling of Ojovan et al. [23]. The volume of the individual effluents collected and measured at the jth time interval is v_j, where

$$V(t) = \sum_{t=j} v_j. \tag{2}$$

The total effluent collected, $V(t)$, after 8.57 years (3129 days) was 253.9 L. The amount of radionuclide i, expressed as β/γ, leached out of the waste glass was calculated as $A_i(t)$ in Bq from the following equation:

$$A_i(t) = \sum_{t=j} a_{ij} v_j. \tag{3}$$

The normalized mass loss of radionuclide i, NM_i is then expressed in g/cm^2 from the following equation:

$$NM_i = \frac{A_i(t)}{q_i S}, \tag{4}$$

where S is the surface area of the glass monolith (5.31 cm^2) and $q(i = \beta/\gamma) = 4.96 \times 10^8$ Bq/g. The glass monolith weighed 4.75 g. The leached fraction of ϕ_i, where i is defined as β/γ

$$\Phi_i = \frac{A_i(t)}{A_i(0)}, \tag{5}$$

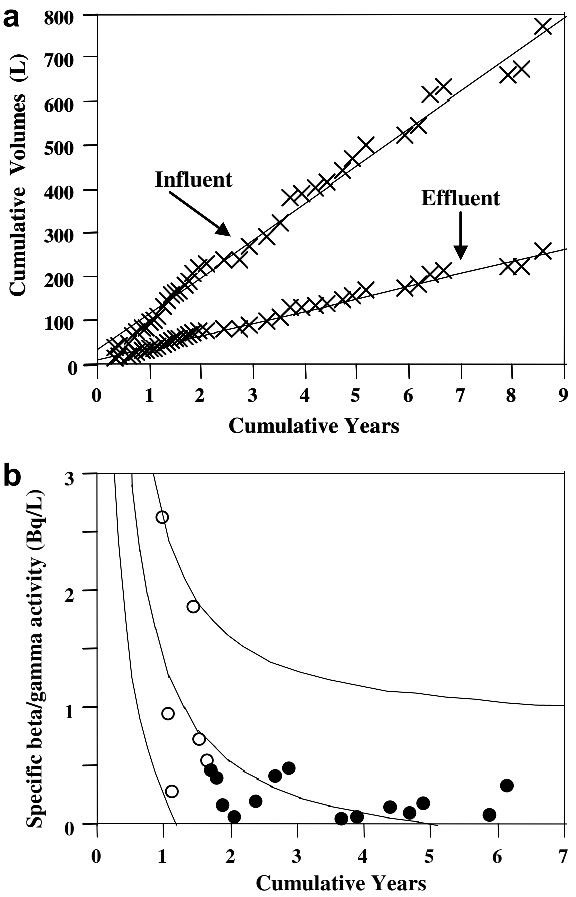

Fig. 6. Cumulative groundwater volume that contacted the radioactive Tank 15 waste glass as a function of time (top) and the specific beta/gamma radioactivity of the groundwater as a function of time (bottom). Open circles represent monthly sampling intervals and solid circles represent quarterly sampling intervals.

where $A_{\beta/\gamma}(0) = 2.36 \times 10^9$ Bq is the total activity in the Tank 15 glass at burial.

Fig. 7 shows the normalized mass loss and leached fraction of β/γ with time.

The average normalized leaching rate of radionuclide i, NR_i, was calculated using

$$\mathrm{NR}_i = \frac{\mathrm{NM}_i}{t},$$

where t is the duration of the test in days.

Fig. 8 (top) shows the normalized leaching rate as a function of time. It can be seen from Fig. 8 (top) that the overall leaching rate of β/γ progressively diminished with time resulting in a rate that is a half order of magnitude smaller than the initial rate after 8 years of burial. This is an intrinsic characteristic of a diffusion controlled process rather than a glass matrix dissolution via hydrolysis. The latter mechanism would show a constant leaching rate. Since Fig. 8 (top) follows a square root dependency with time it indicates an ion exchange mechanism of glass corrosion rather than a linear hydrolysis mechanism [23] which is expected for the β/γ components in Table 2. The bottom of Fig. 8 shows the time dependence of the normalized mass losses of β/γ divided by the square root of time ($\mathrm{NM}_i/\sqrt{t}$). Fig. 8 (bottom) demonstrates that this ratio remains almost constant over the 8 years duration of the lysimeter measurements, which indicates that the β/γ are released from the Tank 15 glass via a diffusion controlled process. This is consistent with data from burial studies of low-level vitrified wastes [23,75].

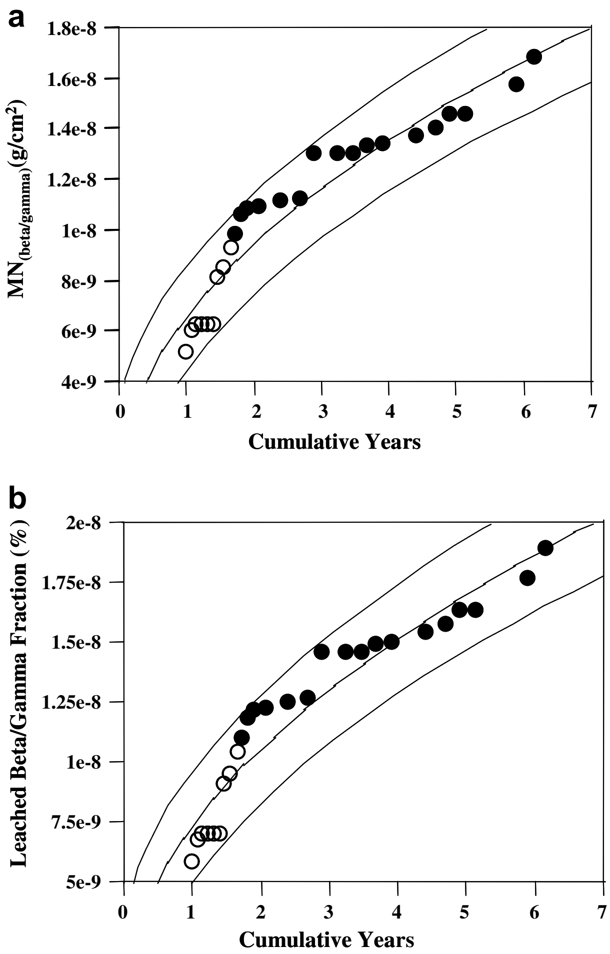

Fig. 7. Normalized mass losses (top) and leached fraction of beta/gamma (bottom) from Tank 15 glass. Open circles represent monthly sampling intervals and solid circles represent quarterly sampling intervals.

In order to calculate an instantaneous leach rate, NR_i, in term of gwaste form/m^2 day the surface area of the glass exposed to the volume of leachant and the test duration must also be factored into the calculation as expressed in

$$\mathrm{NR}_i = \frac{c_i(\text{sample})}{(f_i) \cdot (\mathrm{SA}/V) \cdot (t)}, \tag{6}$$

where NRi is the normalized rate ($\mathrm{g}_{\text{waste form}}/\mathrm{m}^2$ day), SA/V is the surface area of the waste form divided by the leachant volume (m^2/L) and t is the time duration of the test (days).

4.6. Prediction of the resumption of dissolution (Stage III)

A new approach [30] based on Activated Complex Theory (ACT™), was used to predict the return to the forward rate (Stage III) behavior for the burial glass compositions in Table 1. The CRNL glass is excluded from this analysis as it is an aluminosilicate glass and not a borosilicate glass and the approach has only been investigated for borosilicate based waste glasses.

This approach is based on mineral moieties (clusters) in borosilicate waste glasses. The concentration of mineral moieties such as albite ($\mathrm{NaAlSi_3O_8}$), jadeite ($\mathrm{NaAl_2Si_2O_6}$), nepheline ($\mathrm{NaAlSiO_4}$), and acmite ($\mathrm{NaFeSi_2O_6}$) in a glass are determined from the glass composition. These compositions can be expressed on a ternary phase diagram composed of the end members Si, Al, and Fe in at.% when there is sufficient alkali in the glass to form any of the mineral moieties. Such a ternary is shown in Fig. 9 and was developed using

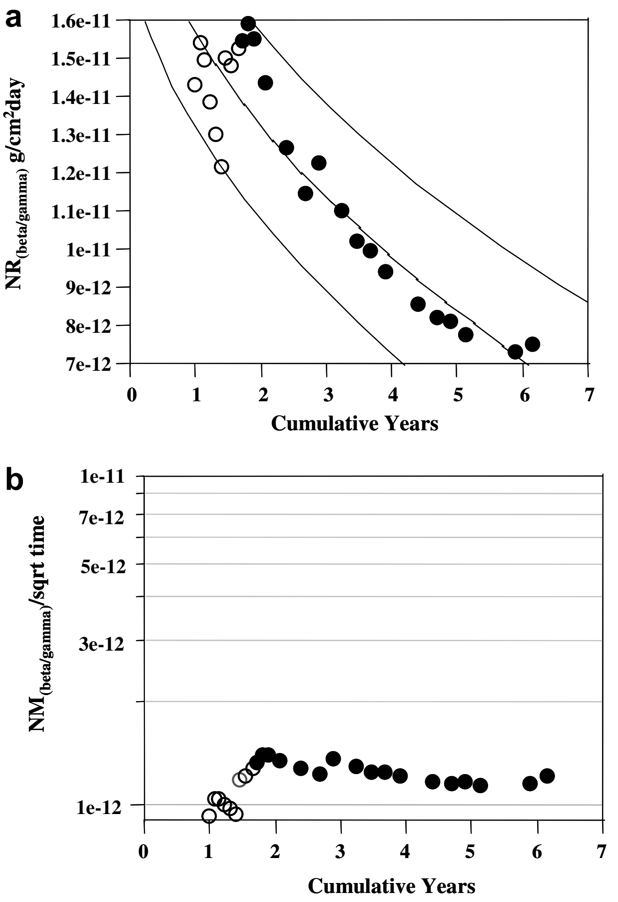

Fig. 8. Average normalized leaching rates (top) based on β/γ and normalized mass loses divided by square root of time (bottom) for Tank 15 glass. Open circles represent monthly sampling intervals and solid circles represent quarterly sampling intervals.

217 glass compositions. The compositions of the Belgian/French, Russian, and US burial glasses are overlain on Fig. 9.

Fig. 9 demonstrates that glasses with high concentrations of albite (Ab) and acmite (Ac) are predicted to form ferrosilicate clay minerals on the leached glass surface and these glasses should not return to the forward rate because aluminosilicate phases are not predicted to form. Glasses with low Ab have more jadeite (Jd) and insufficient Si to form acmite. In other words, the Al:Si ratio of the glass and the activated surface complexes are more favorable to the formation of analcime (zeolite) which has the same Al:Si ratio as Jd. The glasses with more Jd component are thus more likely to return to the forward rate of dissolution (Stage III). Most of the Belgium/French, and the Russian and US burial glasses all have sufficient Si (at.%) to maintain steady state dissolution. Only the SAN60 and SM527 glasses are predicted to return to the forward rate (Stage III dissolution) and both SAN 60 [1] and SM527 [76] have been experimentally shown to do so.

The reaction of the mineral moieties in each glass can also be examined on a thermodynamic basis. If a glass is primarily an albite glass it cannot form analcime by reaction with water as the free energy of the reaction is not energetically favored, e.g. the free energy of formation of Eq. (3) at 90 °C is +23.5 kJ/mol

$$\underbrace{NaAlSi_3O_8}_{\text{albite}} + H_2O \overset{90\,^{\circ}C}{\rightarrow} \underbrace{NaAlSi_2O_6 \cdot H_2O}_{\text{analcime}} + SiO_2(aq). \tag{7}$$

If a glass is primarily jadeite it is energetically favored ($\Delta G_{fm} = -9.8$ kJ/mol at 90 °C) to form when reacted with water (Eq. (8)). Note also that the Al:Si ratio of Jd and analcime are the same so it is also structurally favored.

$$\underbrace{NaAl_2Si_2O_6}_{\text{jadeite}} + H_2O \overset{90\,^{\circ}C}{\rightarrow} \underbrace{NaAlSi_2O_6 \cdot H_2O}_{\text{analcime}}. \tag{8}$$

If a glass is primarily nepheline, a source of aqueous SiO_2 is needed for the formation of analcime in addition to H_2O (Eq. (8)) and the reaction is energetically favored ($\Delta G_{fm} = -38.2$ kJ/mol at 90 °C)

$$\underbrace{NaAlSiO_4}_{\text{nepheline}} + H_2O + SiO_2(aq) \overset{90^{\circ}\,C}{\rightarrow} \underbrace{NaAlSi_2O_6 \cdot H_2O}_{\text{analcime}}. \tag{9}$$

In the presence of excess OH^-, nepheline glass moieties can form paragonite (Eq. (10)). The formation of paragonite from nepheline is energetically favored ($\Delta G_{fm} = -139$ kJ/mol at 90 °C). In turn, paragonite can form analcime by reaction with more base and a source of aqueous SiO_2 (Eq. (1)) and this is also energetically favored ($\Delta G_{fm} = -170$ kJ/mol at 90 °C).

$$\underbrace{3NaAlSiO_4}_{\text{nepheline}} + 2OH^- \overset{90\,^{\circ}C}{\rightarrow} \underbrace{NaAl_3Si_3O_{10}(OH)_2}_{\text{paragonite}} + 2Na^+, \tag{10}$$

$$\underbrace{NaAl_3Si_3O_{10}(OH)_2}_{\text{paragonite}} + 2NaOH(aq) + 3SiO_2(aq) \overset{90^{\circ}\,C}{\rightarrow} \underbrace{3NaAlSi_2O_6 \cdot H_2O}_{\text{analcime}} + H_2O. \tag{11}$$

However, if a glass has sufficient acmite in it and enough of an albite component then it is highly energetically favored ($\Delta G_{fm} = -604$ kJ/mol at 90 °C) to form nontronite (a Fe-rich clay mineral) and continue to leach at steady state rate (Eq. (12)). No excess aqueous SiO_2 is needed for this reaction to occur.

$$\underbrace{2NaFeSi_2O_6}_{\text{acmite}} + \underbrace{0.33NaAlSi_3O_8}_{\text{albite}} + 2H_2O \overset{90\,^{\circ}C}{\rightarrow} \times \underbrace{Na_{0.33}Fe_2Al_{0.33}Si_{3.67}O_{10}(OH)_2}_{\text{nontronite}} + 1.32SiO_2(aq) + 2NaOH. \tag{12}$$

Thus glasses with insufficient Si to form albite moieties, will form jadeite or nepheline moieties that are more susceptible to forming analcime and returning to the forward rate of dissolution via Eqs. (8)–(11) than glasses with sufficient Si to form albite and sufficient Fe to form acmite (Eqs. (7) and (12)). Eq. (12) is the most likely reaction stabilizing an iron containing glass, like Tank 15 SRS glass, at steady state (Stage II) dissolution.

5. Conclusions

The Tank 15 HLW burial glass was found to be very durable in both the burial environment and during accelerated laboratory durability testing. Surface layer formation was minimal and the surface layer was enriched in both Al and Fe. The surface layer structure was simple, depletion in alkali and alkaline earth and enrichment in Al, Si, and Fe structural elements. Modeling the glass composition using ACT™ and noting that the surface layer is enriched in Fe suggests that this glass will not return to the forward rate of dissolution (Stage III) but continue to leach at a steady state rate.

The Tank 15 HLW burial glass was predicted to be durable using two different SRNL durability models (THERMO™ and ACT™) based on short term and long term durability testing with ASTM C1285 (Product Consistency Test). Short term durability measurement of the burial glass confirmed this.

Only ^{137}Cs and ^{90}Sr and their radioactive daughters ^{137m}Ba and ^{90}Y in the Tank 15 HLW glass were detected in the lysimeter leachates and in the soil. No alpha radiation from the Pu in the glass was

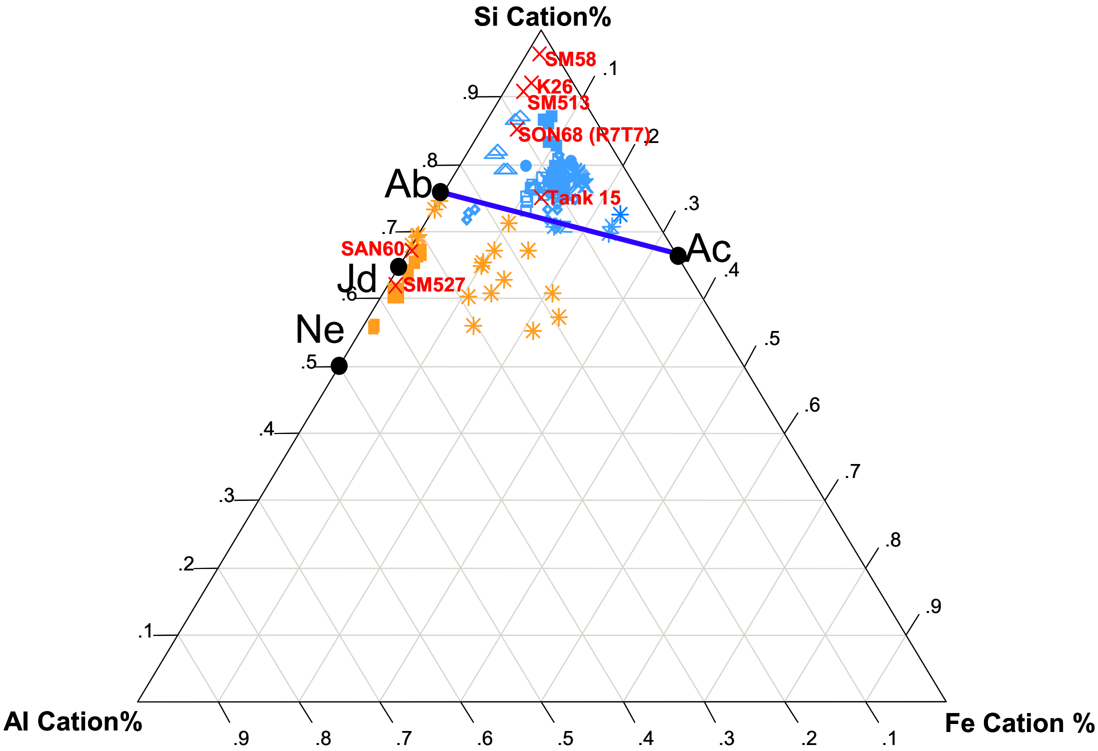

Fig. 9. Predicted performance of the burial glasses in terms of the return to the forward rate. Glasses below the Albite (Ab)-Acmite (Ac) join are predicted to form analcime or paragaonite and return to the forward rate (Stage III) while glasses above the Ab-Ac join are predicted to form nontronite clays and/or ferrite phases and leach at steady state (Stage II) rates. Note that the Canadian (CRNL) glasses are not included as they are not borosilicate glasses and this methodology has not been proven to apply to aluminosilicate glasses.

detected in either the leachates or the soil. The mechanism of leaching of the beta/gamma radiation appeared to be diffusion controlled. The ^{137}Cs and ^{90}Sr that leached from the glass that were found in the soil were presumably bound by iron oxyhydroxides in the soil column as found in the Belgian and Canadian burial studies. Superior or equivalent performance of burial glasses in unsaturated and saturated sediments compared to saturated accelerated laboratory tests is consistent with other long term radioactive burial experiments in Canada, Belgium, and Russia.

Acknowledgements

The authors would like to thank Dr S.B. Clark of the Washington State University for her contribution to the early portion of this study. The authors would also like to acknowledge the assistance and support of Dr G.G. Wicks of SRNL without whose assistance this publication may not have been completed. This research was sponsored by the Department of Energy (EM-50) by an Independent Research & Development (IR&D-2004) grant in connection with work done under Contract No. DE-AC09-96SR18500 with the US Department of Energy. Since the burial studies were initiated in 1981 and the documentation completed in 2008 the work was performed under Contract Nos. DE-AC09-76SR00001, DE-AC09-89SR18035, and DE-AC-09-96SR18500 with the US Department of Energy.

References

[1] P. Van Iseghem, B. Grambow, in: J.J. Apted, R.E. Westerman (Eds.), Science Basis for Nuclear Waste Management XI, Materials Research Society, Pittsburgh, PA, 1987, p. 631.
[2] Y. Inagaki, K. Idemitsu, T. Arima, T. Maeda, H. Ogawa, F. Itonaga, in: B.P. McGrail, G.A. Cragnoliono (Eds.), Scientific Basis for Nuclear Waste Management XXV, Materials Research Society, Pittsburgh, PA, 2002, p. 589.
[3] T.A. Abrajano, J.K. Bates, C.D. Byers, J. Non-Cryst. Solids 84 (1986) 251.
[4] W.L. Ebert, Defense High Level Waste Glass Degradation, Office of Civilian Radioactive Waste Management Analysis/Model, ANL-EBS-MD-000016, Rev.00 ICN01, 2000.
[5] W.L. Ebert, Ceramic Transactions, vol. 143, American Ceramic Society, Westerville, OH, 2003. p. 235.
[6] G.G. Wicks, J. Nucl. Mater. 298 (2001) 78.
[7] G.G. Wicks, in: D.E. Clark, B.K. Zoitos (Eds.), Corrosion of Glass, Ceramics, and Ceramic Superconductors, Noyes Publications, Park Ridge, NJ, 1992, p. 218.
[8] P. Van Iseghem, in: Scientific Basis for Nuclear Waste Management XVII, Materials Research Society Symposium Proceedings, vol. 333, 1994, p. 133.
[9] R.J. Hand, J. Glass Sci. Technol. Part A 46 (3) (2005) 237.
[10] A. Lodding, P. Van Iseghem, J. Nucl. Mater. 298 (2001) 97.
[11] P. Van Iseghem, E. Valcke, A. Lodding, J. Nucl. Mater. 298 (2001) 86.
[12] E. Valcke, S. Smets, S. Labat, K. Lemmens, P. Van Iseghem, P. Thomas, N. Godon, P. Jollivet, G. Parisot, J. Mestre, N. Jockwer, K. Wieczorek, C. Pozo, Mat. Res. Soc. Symp. Proc. 932 (2006) 67.
[13] E. Valcke, M. Gysemans, H. Moors, P. Van Iseghem, N. Godon, P. Jollivet, Mat. Res. Soc. Symp. Proc. 932 (2006) 999.
[14] W.F. Merritt, The Leaching of Radioactivity from Highly Radioactive Glass Blocks Buried Below the Water Table: Fifteen Years of Results, Atomic Energy of Canada Ltd. Report No. AECL-5317, Ontario, Canada, 1976.
[15] A.R. Bancroft, J.D. Gamble, Initiation of a Field Burial Test of the Disposal of Fission Products Incorporated into Glass, Atomic Energy of Canada Ltd. Report No. AECL-718, Ontario, Canada, 1978.
[16] T.W. Melnyk, F.B. Walton, L.H. Johnson, Nucl. Chem. Waste Manage. 5 (1984) 49.
[17] J.C. Tait, W.H. Hocking, J.S. Betteridge, G. Bart, in: D.E. Clark, W.B. White, A.J. Machiels (Eds.), Advances in Ceramics, Nuclear Waste Management II, vol. 20, American Ceramic Society, Columbus, OH, 1986, p. 559.
[18] W.F. Merritt, Permanent disposal by burial of highly radioactive wastes incorporated into glass, in: Proceedings of a Symposium on the Disposal of Radioactive Wastes into the Ground, International Atomic Energy Agency (IAEA) May 29–June 2, 1967, p. 403.
[19] M.I. Ojovan, N.V. Ojovan, I.V. Startceva, G.N. Chuikova, A.S. Barinov, Mater. Res. Soc. Symp. Proc. V 663 (2001) 837.
[20] M.I. Ojovan, W.E. Lee, A.S. Barinov, I.V. Startceva, D.H. Bacon, B.P. McGrail, J.D. Vienna, Glass Technol. 47 (2) (2006) 48.
[21] B.P. McGrail, D.H. Bacon, P.D. Meyer, M.I. Ojovan, D.M. Strachan, N.V. Ojovan, I.V. Startceva, Mater. Res. Soc. Symp. Proc. V 757 (2003) 83.
[22] M.I. Ojovan, N.V. Ojovan, I.V. Startceva, G.N. Tchuikova, Z.I. Golubeva, A.S. Barinov, J. Nucl. Mater. 298 (2001) 174.
[23] M.I. Ojovan, R.J. Hand, N.V. Ojovan, W.E. Lee, J. Nucl. Mater. 340 (2005) 12.
[24] I.A. Sobolev, M.I. Ojovan, O.G. Batyukhnova, N.V. Ojovan, T.D. Scherbatova, Mater. Res. Soc. Symp. V 465 (1997) 245.

[25] N.V. Ojovan, I.V. Sartceva, A.S. Barinov, A.V. Mokhov, M.I. Ojovan, G. Mobus, Mater. Res. Soc. Symp. Proc. V 807 (2004) 139.
[26] C.M. Jantzen, J.B. Pickett, K.G. Brown, T.B. Edwards, US Patent #5,846,278, Method of Determining Glass Durability (THERMO™), 1998.
[27] C.M. Jantzen, J.B. Pickett, K.G. Brown, T.B. Edwards, D.C. Beam, Process/Product Models for the Defense Waste Processing Facility (DWPF): Part I. Predicting Glass Durability from Composition Using a Thermodynamic Hydration Energy Reaction MOdel (THERMO), US DOE Report WSRC-TR-93-0672, 1995, p. 464.
[28] C.M. Jantzen, K.G. Brown, in: V.G.T. Chandler (Ed.), Environmental Issues and Waste Management Technologies in the Ceramic and Nuclear Industries, Ceramic Transactions, vol. 107, 2000, p. 289.
[29] ASTM C1285, Standard Test Methods for Determining Chemical Durability of Nuclear, Hazardous, and Mixed Waste Glasses and Multiphase Glass Ceramics: The Product Consistency Test (PCT), Annual Book of ASTM Standards, vol. 12.01, 2002.
[30] C.M. Jantzen, J.M. Pareizs, Glass Durability Modeling: Application of Activated Complex Theory (ACT) for High Level Waste (HLW) Glass Melter Process Control, WSRC-TR-2005-00317 (in revision for J. Nucl. Mater.).
[31] P. VanIseghem, M. Aertsens, S. Gin, D. Deneele, B. Grambow, P. McGrail, D. Strachan, G. Wicks, GLAMOR, A Critical Evaluation of the Dissolution Mechanisms of High Level Waste Glasses in Conditions of Relevance for Geological Disposal, EUR23097, 2007.
[32] R.W. Douglas, T.M.M. El-Shamy, J. Am. Ceram. Soc. 50 (1) (1967) 1.
[33] J.E. Mendel (Compiler), Final Report of the Defense High-Level Waste Leaching Mechanisms Program, US DOE Report PNL-5157, Battelle Pacific Northwest Laboratories, Richland WA, 1984.
[34] L.L. Hench, D.E. Clark, Surface Properties and Performance Prediction of Alternative Waste Forms, NUREG/CR-3472, vol. 2, 1986.
[35] C.M. Jantzen, in: D.E. Clark, B.K. Zoitos (Eds.), Corrosion of Glass, Ceramics, and Ceramic Superconductors, Noyes Publications, Park Ridge, NJ, 1992, p. 153.
[36] R.M. Wallace, G.G. Wicks, in: D.G. Brookins (Ed.), Scientific Basis for Nuclear Waste Management, Elsevier North Holland, New York, 1983, p. 23.
[37] G.G. Wicks, W.C. Mosley, P.G. Whitkop, K.A. Saturday, J. Non-Cryst. Solids 49 (1982) 413.
[38] C.M. Jantzen, D.R. Clarke, P.E.D. Morgan, A.B. Harker, J. Am. Ceram. Soc. 65 (6) (1982) 292.
[39] A. Gauthier, P. LeCoustumer, J.-H. Thomassin, in: B.P. McGrail, G.A. Cragnoliono (Eds.), Scientific Basis for Nuclear Waste Management XXV, Materials Research Society, Pittsburgh, PA, 2002, p. 555.
[40] L.L. Hench, D.E. Clark, J. Non-Cryst. Solids 28 (1978) 83.
[41] A.B. Woodland, J.K. Bates, T.J. Gerding, Parametric Effects on Glass Reaction in the Unsaturated Test Method, US DOE Report ANL-91/36, Argonne National Laboratory, Argonne, IL, 1991, p. 130.
[42] J.K. Bates, C.R. Bradley, E.C. Buck, J.C. Cunnane, N.L. Dietz, W.L. Ebert, J.W. Emery, R.C. Ewing, X. Feng, T.J. Gerding, M. Gong, W.-T Han, J.C. Hoh, J.J. Mazer, M. Tomozawa, L.-M. Wang, D.J. Wronkiewicz, ANL Technical Support Program for DOE Environmental Restoration and Waste Management, Annual Report October 1990–September 1991, US DOE Report ANL-92/9, Argonne National Laboratory, Argonne, IL, 1992, p. 149.
[43] X. Feng, J.C. Cunnane, J.K. Bates, in: G.B. Mellinger (Ed.), Ceramic Transactions, vol. 39, American Ceramic Society, Westerville, OH, 1994, p. 341.
[44] A.K. Bandyopadhyai, R. Jabra, J. Phalippou, J. Mater. Sci. Lett. 8 (12) (1989) 1464.
[45] A.B. Woodland, J.K. Bates, T.J. Gerding, Parametric Effects on Glass Reaction in the Unsaturated Test Method, US DOE Report ANL-91/36, Argonne National Laboratory, Argonne, IL, 1991, p. 130.
[46] J.K. Bates, C.R. Bradley, E.C. Buck, J.C. Cunnane, N.L. Dietz, W.L. Ebert, J.W. Emery, R.C. Ewing, X. Feng, T.J. Gerding, M. Gong, W.-T Han, J.C. Hoh, J.J. Mazer, M. Tomozawa, L.-M. Wang, D.J. Wronkiewicz, ANL Technical Support Program for DOE Environmental Restoration and Waste Management, Annual Report October 1990–September 1991, US DOE Report ANL-92/9, Argonne National Laboratory, Argonne, IL, 1992, p. 149.
[47] D.J. Wronkiewicz, J.K. Bates, E.C. Buck, J.C. Hoh, J.W. Emery, L.M. Wang, Radiation Effects in Moist-Air Systems and the Influence of Radiolytic Product Formation on Nuclear Waste Glass Corrosion, US DOE Report ANL-97/15, Argonne National Laboratory, Argonne, IL, 1997.
[48] E.C. Buck, J.A. Fortner, J.K. Bates, X. Feng, N.L. Dietz, C.R. Bradley, B.S. Tani, in: A. Barkatt, R.A. VanKonynenburg (Eds.), Analytical Electron Microscopy Examination of Solid Reaction Products in Long-Term Tests of SRL 200 Waste Glasses, Scientific Basis for Nuclear Waste Management. XVII, Materials Research Society, Pittsburgh, PA, 1994, p. 585.
[49] J.S. Luo, T.A. Abrajano, Jr., W.L. Ebert, Natural Analogues of Nuclear Waste Glass Corrosion, US DOE Report ANL-98/22, Argonne National Laboratory, Argonne, IL, 1998.
[50] B.H.W.S. deJong, C.M. Schramm, V.E. Parziale, Geochim. Cosmochim. Acta 47 (1983) 1223.
[51] L.L. Ames, L.B. Sand, Am. Mineral. 43 (1958) 461.
[52] R. Roy, L.B. Sand, Am. Mineral. 41 (1956) 505.
[53] R. Roy, E.F. Osborn, Am. Mineral. 39 (1954) 853.
[54] R.A. Sheppard, Zeolitic Diagenesis of Tuffs in the Miocene Chalk Hills Formation, Western Snake River Plain, Idaho, US Geological Survey Bulletin, 1963, p. 27.
[55] A.F. White, J. Non-Cryst. Solids 67 (1984) 225.
[56] R.A. Sheppard, A.J. Gude, Distribution and Genesis of Authigenic Silicate Minerals in Tuffs of Pleistocene Lake Tecopa, Inyo County, California, US Geol. Survey Prof. Paper 597, 1968, p. 38.
[57] D. Savage, N.A. Chapman, Chem. Geol. 36 (1982) 59.
[58] J.K. Bates, C.R. Bradley, N.L. Dietz, W.L. Ebert, J.W. Emery, T.J. Gerding, J.C. Hoh, J.J. Mazer, J.E. Young, Unsaturated Glass Testing for DOE Program in Environmental Restoration and Waste Management, Annual Report, October 1989–September 1990, US DOE Report ANL-90/40, Argonne National Laboratory, Argonne, IL, 1991.
[59] M.E. Morgenstein, D.L. Shettel, Jr., Evaluation of borosilicate glass as a high-level radioactive waste form, high level radioactive waste management, in: Proceedings of the Fourth Annual International Conference, vol. 2, Am. Nucl. Soc., La Grange Park, IL, 1993, p. 1728.
[60] R.C. Ewing, in: I.G.J. McCarthy (Ed.), Scientific Basis for Nuclear Waste Management, Plenum, New York, 1979. p. 57.
[61] G. Malow, W. Lutze, R.C. Ewing, J. Non-Cryst. Solids 67 (1984) 305.
[62] C.C. Allen, in: V.W. Lutze (Ed.), Science Basis for Nuclear Waste Management, Elsevier Science Publishing, New York, 1982, p. 37.
[63] C.M. Jantzen, M.J. Plodinec, J. Non-Cryst. Solids 67 (1984) 207.
[64] W.L. Bourcier, D.W. Peiffer, K.G. Knauss, K.D. McKeegan, D.K. Smith, in: V.M. Oversby, P.W. Brown (Eds.), Scientific Basis for Nuclear Waste Management, XIII, vol. 176, Materials Research Society, Pittsburgh, PA, 1990, p. 209.
[65] Y. Inagaki, K. Idemitsu, T. Arima, T. Maeda, H. Ogawa, F. Itonaga, in: B.P. McGrail, G.A. Cragnoliono (Eds.), Scientific Basis for Nuclear Waste Management, XXV, Materials Research Society, Pittsburgh, PA, 2002, p. 589.
[66] W.L. Ebert, J.K. Bates, C.R. Bradley, E.C. Buck, N.L. Dietz, N.R. Brown, Ceramic Transactions, vol. 39, American Ceramic Society, Westerville, OH, 1994, p. 333.
[67] D.H. Bacon, M.I. Ojovan, B.P. McGrain, N.V. Ojovan, I.V. Startsceva, Am. Soc. Mater. Eng. (2003).
[68] G.B. Woolsey, R.M. Galloway, M.J. Plodinec, E.L. Wilhite, J.R. Fowler, Processing of Tank 15 Sludge, USDOE Report DPST-80-361, Savannah River Laboratory, E.I. DuPont deNemours & Co., Aiken, SC, 1980.
[69] J.A. Stone, Separation of SRP Waste Sludge and Supernate, USDOE Report DP-1441, Savannah River Laboratory, E.I. DuPont deNemours & Co., Aiken, SC, 1976.
[70] C.M. Jantzen, N.E. Bibler, D.C. Beam, M.A. Pickett, Characterization of the Defense Waste Processing Facility (DWPF) Environmental Assessment (EA) Glass Standard Reference Material, US DOE Report WSRC-TR-92-346, Rev. 1, Westinghouse Savannah River Company, Aiken, SC, 1993.
[71] C.M. Jantzen, N.E. Bibler, D.C. Beam, M.A. Pickett , Environmental and Waste Management Issues in the Ceramic Industry, Ceramic Transactions, vol. 39, American Ceramic Society, Westerville, OH, 1994, p. 313.
[72] G.L. Smith, Characterization of Analytical Reference Glass-1 (ARG–1), US DOE Report PNL–8992, Pacific Northwest National Laboratory, Richland, WA, 1993.
[73] N.E. Bibler, C.J. Bannochie, J.W. Ray, in: Waste Management '06 Proceedings, WM Symposia Inc., Tucson, AZ, 2006.
[74] V. Pirlet, J. Nucl. Mater. 298 (2001) 47.
[75] B.P. McGrail, J.P. Icenhower, D.K. Shuh, P. Liu, J.G. Darab, D.R. Baer, S. Thevuthasen, V. Shutthanandan, M.H. Engelhard, C.H. Booth, P. Nachimuthu, J. Non-Cryst. Solids 296 (2001) 10.
[76] K. Lemmens, J. Nucl. Mater. 298 (2001) 11.
[77] M.I. Ojovan, O.G. Batyukhova, S.A. Dmitriev, A.S. Barinov, I.V. Startceva, An Assessment of Radionuclide Release Inventory Based on Long-Term Field Tests of Nuclear Waste glass K-26, ICEM05-1067, 2005.
[78] T. Advocat, P. Jollivet, J.L. Crovisier, M. DelNero, J. Nucl. Mater. 298 (2001) 55.
[79] C.M. Jantzen, K.G. Brown, Ceram. Trans. V 107 (2000) 289.
[80] D.K. Bailey, J.F. Schairer, J. Petrol. 7 (1) (1966) 114.
[81] I. Hager, M. Hahnert, W. Hinz, Silikatechnik 18 (11) (1967) 360.
[82] J.A. Topping, M.K. Murthy, J. Am. Ceram. Soc. 56 (5) (1973) 270.